Theor Chem Account (2008) 119:297–303
DOI 10.1007/s00214-007-0383-6

REGULAR ARTICLE

Theoretical studies on the mechanisms of NCCO + O_2 reaction

Yi-Zhen Tang · Jing-Yu Sun · Hao Sun · Ya-Ru Pan · Rong-Shun Wang

Received: 15 May 2007 / Accepted: 16 July 2007 / Published online: 18 August 2007

Abstract The mechanisms of the reaction of NCCO with molecular oxygen are investigated at the G3MP2//B3LYP/6-311G(d,p) levels for the first time. The calculation results show that two mechanisms are involved, namely, O attack on α-C atom mechanism and O attack on β-C atom mechanism, with six products yielded. The most feasible channel is the addition of O_2 to β-C atom in NCCO radical leading to the energy-rich intermediate IM1, NCC(O)OO, which can isomerize to a four-center-structure IM3, and then undergoes C–C and O–C bond fission to form P1(NCO + CO_2) finally. The barriers are 27.3 and 25.4 kcal/mol, respectively. For other channels involved in the two mechanisms, with less stable initial adducts and higher barrier, they are less conceivable dynamically and thermochemically.

Keywords NCCO · O_2 · Transition state · Mechanism

1 Introduction

Nitrogen–oxygen carbon chain molecules NC_nO, similar to elemental composition of the well-known C_nO and C_nN identified in interstellar space, are very important in various aspects [1–3]. One particular interest is their possible role in astrophysical chemistry [4–7]. Moreover, NCCO can be seen as one of the important intermediates in combustion and the nitric oxide reburning processes [7,8]. Therefore, NCCO has been considered as potential interstellar molecule and important target in astronomical research, and received experimental and theoretical attentions extensively [9–14]. It has been established that NCCO radical and ismoers are the major product in gas phase photodissociation of carbonylcyanide ($CO(CN)_2$) by photofragment translational energy spectroscopy [9]. High level ab initio calculations were carried out on NCCO and $NCCO^+$ by Francisco and Liu [11]. Yu et al. [12] studied the stability and prosperities of the NCCO isomers.

The reaction of NCCO radical with O_2 had been investigated by Imamura and Washida [14], and the rate constants were determined, but no products were given. In their paper, NCCO was generated by photodissociation of acetylcyanide. Rate constants were determined by measuring the decay rates of the time dependence of the radical concentrations. To our best knowledge, there is no theoretical study on the title reaction until now. So in our work, the mechanisms of the title reaction are investigated in order to identify the pathways and products, and expect it will be helpful for further experimental and theoretical research.

In this paper, the pathways of NCCO + O_2 reaction have been investigated using density function theory and ab initio methods. For the title reaction, the following product channels are revealed for the first time, i.e.,

$$\text{NCCO} + O_2 \rightarrow \text{NCO} + CO_2 + 113.3\,\text{kcal/mol} \quad (1)$$
$$\rightarrow \text{CNO} + CO_2 + 50.6\,\text{kcal/mol} \quad (2)$$
$$\rightarrow \text{NCO} + \text{CO} + \text{O} - 15.4\,\text{kcal/mol} \quad (3)$$
$$\rightarrow CO_2 + \text{CN} + \text{O} - 27.7\,\text{kcal/mol} \quad (4)$$
$$\rightarrow \text{CO} + \text{ONCO} + 54.4\,\text{kcal/mol} \quad (5)$$
$$\rightarrow 2\text{CO} + \text{NO} + 70.9\,\text{kcal/mol} \quad (6)$$

Y.-Z. Tang · J.-Y. Sun · H. Sun · Y.-R. Pan · R.-S. Wang (✉)
Institute of Functional Material Chemistry,
Faculty of Chemistry, Northeast Normal University,
Renmin Road 5268, Changchun,
Jilin 130024, People's Republic of China
e-mail: wangrs@nenu.edu.cn

2 Computational methods

The geometries of the reactants, products, intermediates, and transition states for the NCCO + O_2 reaction are optimized using the B3LYP theory conjunction with the standard 6-311G(d,p) basis set. For the current reaction involving six heavy atoms, the B3LYP/6-311G (d,p) level of theory is a balanced method in the consideration of computational efficiency and accuracy. Harmonic vibrational frequencies and the zero-point energies (ZPE) corrections are calculated at the same level. The intermediates are characterized by all the real frequencies. The transition states have only one imaginary frequency. Subsequently, Intrinsic reaction coordinate (IRC) calculations are carried out at the B3LYP/6-311G(d,p) level for connecting a transition states to reactants and products.

The energies of the stationary points are calculated using the G3MP2//B3LYP method [15,16], which is a composite scheme based on three single point energies, i.e., QCISD(T)/6-31G(d), MP2/6-31G(d), and MP2/G3MP2 large. The G3MP2//B3LYP total energy is obtained using the following formula:

$$\begin{aligned} E(\text{G3MP2}) = {} & E[\text{QCISD(T)}/6-31\text{G(d)}] \\ & + E[\text{MP2/G3MP2large}] \\ & - E[\text{MP2}/6-31\text{G(d)}] \\ & + E(\text{HLC}) + E(\text{SO}) + E(\text{ZPE}) \end{aligned}$$

where $E(\text{HLC}) = -0.004995n_\alpha - 0.005046n_\beta$; n_α and n_β are the number of α and β valence electrons, respectively, with $n_\alpha \geq n_\beta$. The experimental spin-orbital (SO) corrections are used for atomic species. The ZPE corrections calculated at the B3LYP/6-311G(d,p) level are used directly without scaling because empirically it appears that the ZPE correction at such a level of theory is in good agreement with the experimental values. All calculations are carried out using the Gaussian98 program [17].

3 Results and discussions

The optimized geometries of all stationary points at the B3LYP/6-311G(d,p) level are exhibited in Figs. 1 and 2. The potential energy surfaces (PES) at the G3MP2//B3LYP levels are shown in Figs. 3 and 4. The total and relative energies at the B3LYP/6-311G(d,p) and G3MP2//B3LYP levels are listed in Table 1. The energies used in the discussion are obtained at the G3MP2//B3LYP level unless stated otherwise. The letters of α and β are employed to differentiate the C atom in $NC_\alpha C_\beta O$.

3.1 O attack on β-C atom mechanism

The O atom addition to β-C atom leads to IM1 and IM2 without entrance barrier, and the heat released is 29.3 and 28.7 kcal/mol respectively, which can drive further rearrangement reactions. And a transition state TS1 is discovered to connect IM1 and IM2. The major differences among IM1, TS1 and IM2 are the dihedral angle OOCO, which are 180.0, 83.7 and 0.0° in IM1, TS1 and IM2, respectively. With the barrier of 7.7 kcal/mol, obviously, the interconversion reaction is easy to occur.

As seen from Fig. 3, IM1 can take place three possible conversion reactions. The most favorable one is R $\rightarrow$ IM1 $\rightarrow$ TS2 $\rightarrow$ IM3 $\rightarrow$ TS3 $\rightarrow$ P1(NCO + CO_2). From IM1, another intermediate IM3 is formed via a four-numberring transition state TS2, whose barrier is 27.3 kcal/mol. Subsequently, O–O and C–C bond in IM3 cleave simultaneously with a transition state TS3 of 25.4 kcal/mol, and P1 is yielded, the most stable product on the PES. The second pathway is the closure ring process to generate the five-center-ring intermediate IM4, followed by the C–C and O–O bond disassociations to form P2(CNO + CO_2). The transition states are TS4 and TS5, with the barrier of 43.0 and 9.7 kcal/mol, respectively. The former barrier is a little higher to surpass, suggesting that P2 will be less competitive. P2 also can be produced via other channels which will be discussed later. The last possible channel is more complex than path P1 or P2, and it can be written as R $\rightarrow$ IM1 $\rightarrow$ TS6 $\rightarrow$ IM5 $\rightarrow$ TS7 $\rightarrow$ IM14 + O $\rightarrow$ TS24 + O $\rightarrow$ IM15 + O $\rightarrow$ TS25 + O $\rightarrow$ P3(NCO + CO + O). Interestingly, O atom attacking on α-C atom and N atom approaching to β-C atom leads to IM5, a three-number-ring structure, with the overcome barrier (TS6) of 67.3 kcal/mol, which is the rate-determining step. The O–O bond break in IM5 gives to IM14 + O, and the transition state TS7 is discovered, whose barrier is 19.8 kcal/mol. Notably, IM14 can converse into IM15 with the ring-opening step via a low energy barrier TS24, subsequently, the N–C bond stretches and P3(CO + NCO + O) is formed with the barrier of 16.1 kcal/mol (TS25) on the PES. Due to the high barrier of TS6 and less stable than P1, P3 will not compete with the path P1 described above.

IM2 can extrude one O atom to create IM16 + O via TS8, and this process endothermic by 52.8 kcal/mol. Two feasible scenarios are found from IM16 + O to give P3(CO + NCO + O) and P4(CO_2 + CN + O). The first possible channel is IM16 + O $\rightarrow$ TS27 + O $\rightarrow$ P4(CO_2 + CN + O). The C–C bond in IM16 can rupture to produce CO_2 + CN with the barrier (TS27) is 12.9 kcal/mol, and P4 stands at the point of 18.3 kcal/mol on the PES. The second scenario is that IM16 rearranges to IM17 via TS26 which is 26.8 kcal/mol higher than IM16 on the PES. Once IM17 is formed, its C–O bond disassociates easily to produce P3 surmounting a low-lying barrier of 6.3 kcal/mol. Path P3 can be described as follows:

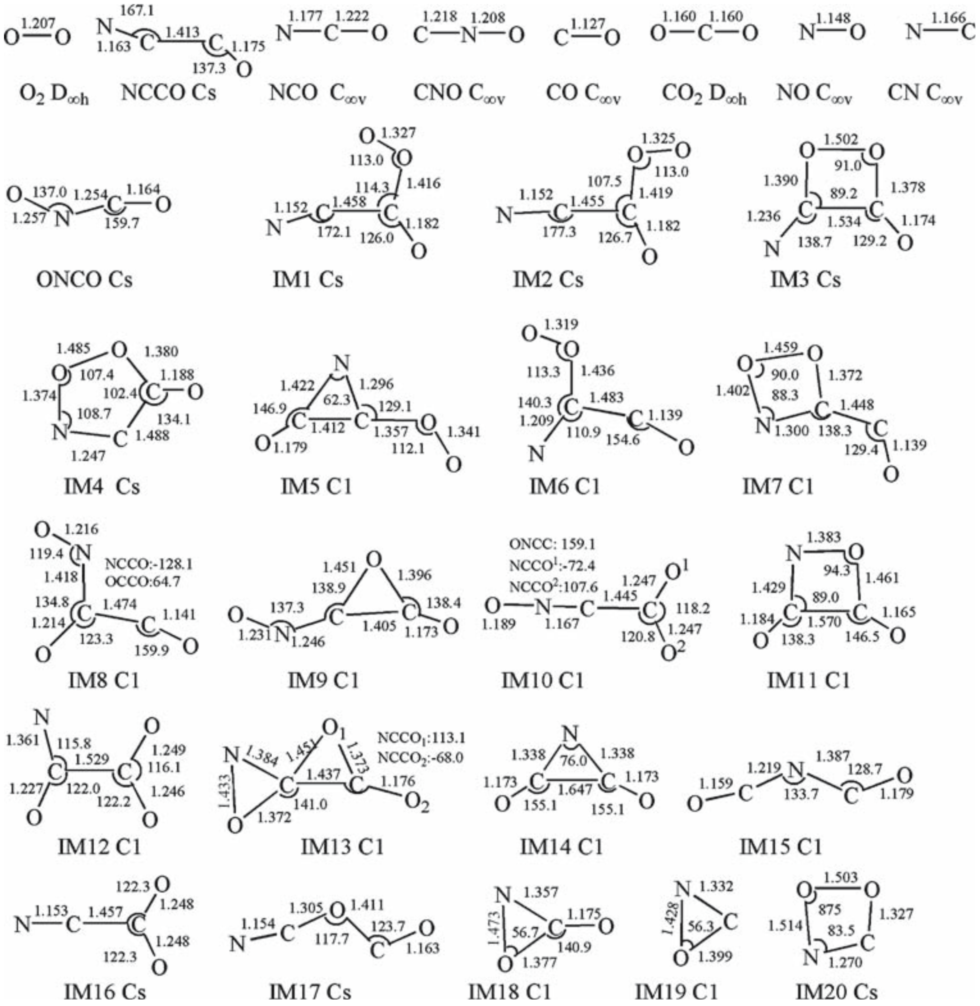

Fig. 1 The optimized geometries of reactants, products and intermediates involved in the NCCO + O_2 reaction at the B3LYP/6-311G(d,p) level (bond length in Å and bond angle in degree)

R → IM1 → TS1 → IM2 → TS8 → IM16 + O → TS26 + O → IM17 + O → TS28 + O → P3(NCO + CO + O). With tight barrier of TS8 and less stable products of P3 and P4, they are dynamically unfeasible compared with path P1 and P2.

3.2 O attack on α-C atom mechanism

According to our calculations, only IM6 is discovered by O_2 interacting with α-C atom in NCCO radical and the transition state TS9 is involved in the process. TS9 is 30.0 kcal/mol higher than reactants. And then a four-number-ring isomer IM7 is formed via TS10, with the barrier of 32.3 kcal/mol. IM6 and IM7 are located at the 16.8 and 18.9 kcal/mol on the PES. Thereafter, IM7 undergoes a N–O bond scission to generate IM8, standing at −36.8 kcal/mol. The transition state is TS11, a very low-energy barrier of 6.8 kcal/mol, and this step released by heat of 55.7 kcal/mol. As for the great amount available energy, many product channels are opened staring from IM8.

The C–C bond in IM8 disassociates directly to give P5(CO + ONCO), whose energy is 57.1 kcal/mol under the recants, and the barrier (TS14) is merely 1.1 kcal/mol. With the very low barrier and stable product, it is conceivable to undergo. Another decomposition scenario of IM8 is the simultaneous cleavage of N–C and C–C bond via TS15, with 7.7 kcal/mol barrier overcome. The final product of this pathway is P6(2CO+NO), and it is exothermic by −84.6 kcal/mol. With lower barrier and more stable product in this mechanism, path P6 is also feasible.

P2 can be produced from the isomerization of IM8. The isomer IM9 can be formed via three-number-ring structure TS12, a latter transition state. Subsequently, IM9 transformes to IM10 involving a ring-opening step. The barrier of the two transition states are 15.6(TS12) and 1.4(TS16) kcal/mol, which are easy to surpass. Subsequently, the C–C bond in IM10 elongates gradually, and P2 is yielded.

IM8 can rearrange to IM11 by the N–O bond rotating around C–N bond, and the corresponding transition state is TS13. The major differences among IM8, TS13 and IM11 are the dihedral angle of ONCO, which are 0.0, 102.9 and

Fig. 2 The optimized geometries of the transition state involved in the NCCO + O_2 reaction at the B3LPY/6-311G(d,p) levels (bond length in Å and bond angle in degree)

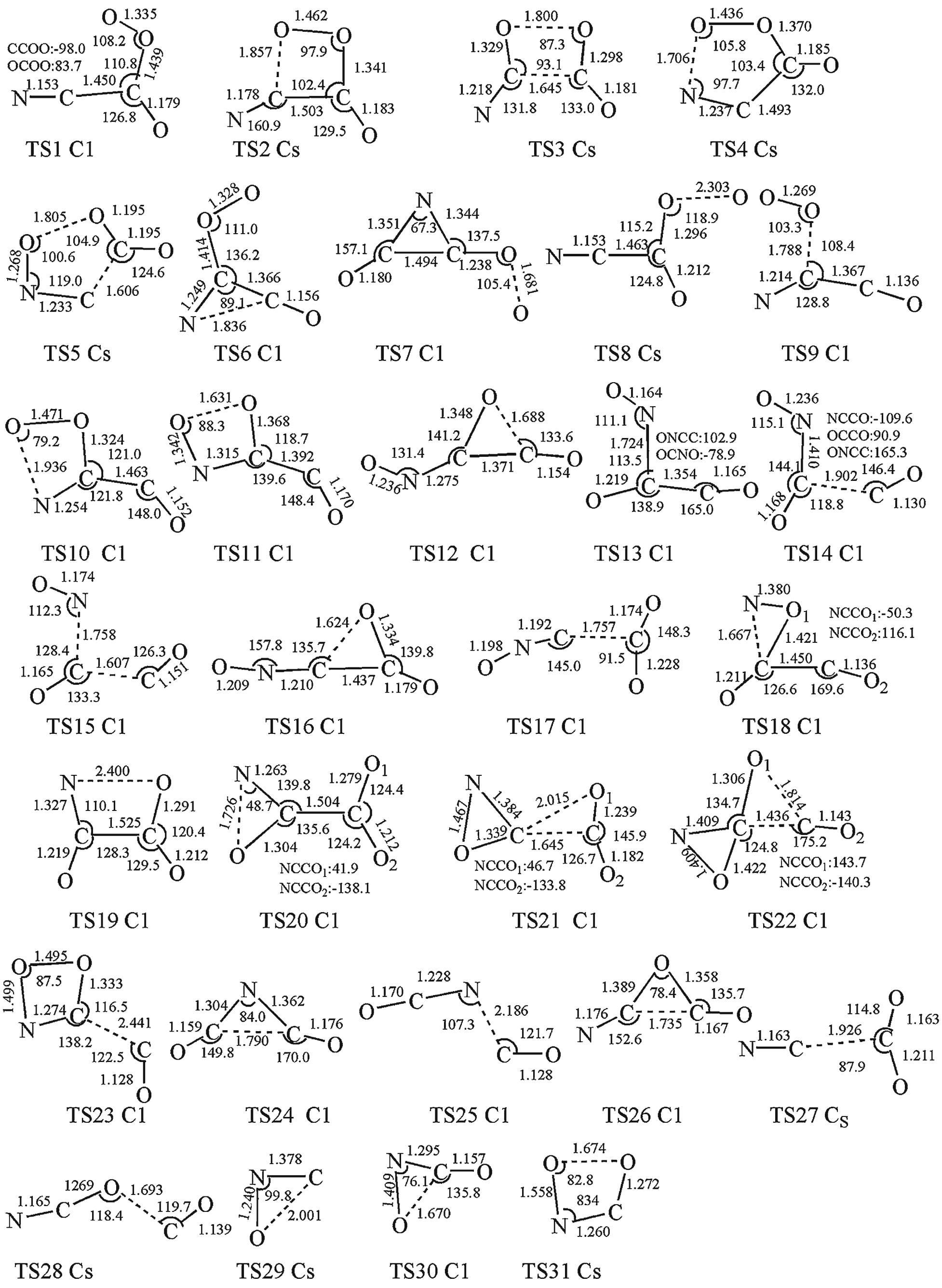

180.0°, respectively. IM11 is the lowest intermediate on the PES, locating at the −62.2 kcal/mol. As seen from Fig. 4, two possible scenarios can occur from IM11 with different products generated. One pathway is that N atom interacts with another C atom leading to the cleavage of C–C bond, and CO + IM18 are yielded. The transition state involved is TS18, 8.7 kcal/mol under than reactants. With a three-number-ring structure, IM18 tends to open the tensional ring. Surmounting a very low barrier of 5.3 kcal/mol (TS30), the line ONCO is obtained. Also, P5 can be formed by another channel which will be described later.

The second feasible channel from IM11 is that N–O bond stretches and then breaks to give out IM12, with a high energy barrier of 67.8 kcal/mol (TS19). The calculations show that IM12 is 50.6 kcal/mol higher than IM11, while −11.6 kcal/mol lower than reactants on the PES. Another adduct IM13 is formed via transition state TS20 with the N atom in IM12 approaching to O atom, and the O1 atom attacking on C atom. The barrier surpassed is 6.7 kcal/mol, and IM13 stands at −21.4 kcal/mol on the PES. IM18 + CO are produced via the low barrier of TS22, whose energy is 8.9 kcal/mol higher than IM13. And then product P5 is

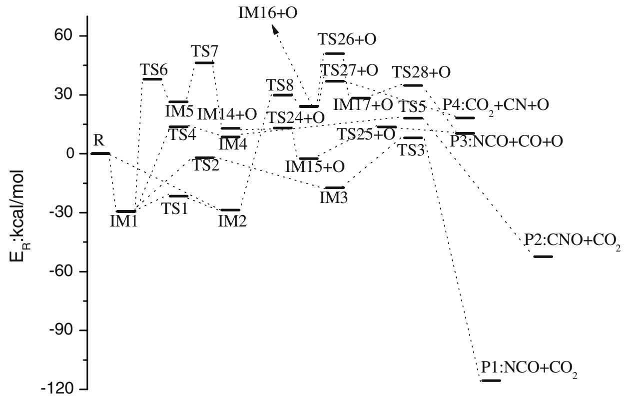

Fig. 3 The NCCO + O_2 reaction potential energy surface of the O attack on β-C atom mechanism at the G3MP2//B3LYP/6-311G(d,p) levels (in kcal/mol)

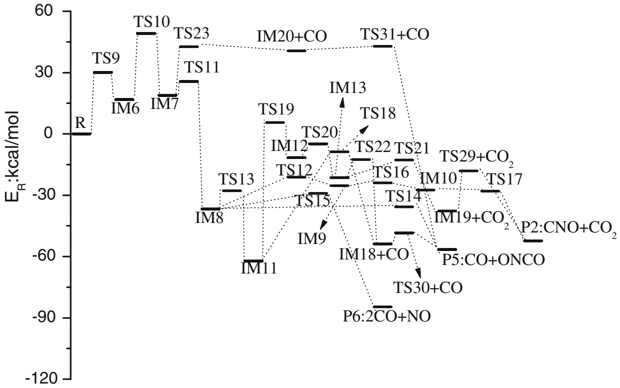

Fig. 4 The NCCO + O_2 reaction potential energy surface of the O attack on α-C atom mechanism at the G3MP2//B3LYP/6-311G(d,p) levels (in kcal/mol)

yielded finally. Or the C–C and C–O bond in IM13 are dissasociated coinstantaneously, with CO_2 + IM19 created. Our results show that IM19 has triangular structure with large tension, and it is transformed to the line structure easily. With the barrier of 19.5 kcal/mol (TS29), CNO is formed, and the termination of this channel is P2(CO_2 + CNO).

It seems that IM11 can dissociate directly in P1(NCO + CO_2), similar to the way IM1 leads to these products. Unfortunately, it is failed to located such a transition state in spite of numerous attempts.

The last channel in this mechanism is the C–C bond fission in IM7 leading to CO molecule and a four-number-ring ONCO (IM20) via TS23, and the barrier is 23.8 kcal/mol. Subsequently, IM20 converses into line structure ONCO, with the very low barrier of 2.2 kcal/mol, and the final product in this channel is P5(CO + ONCO). With the higher energy intermediate and transition states involved, obviously, it makes little contribution to the final product, and can be negligible.

Although IM11 is the lowest intermediate on the whole PES, due to the initial adducts are less stable, and the high-lying and rigid transition state TS9 and TS10, the pathway initiated by O_2 attack on α-C atom is less competitive compared with the O attack on β-C atom mechanism, which is without entrance barrier and highest transition states well below the reactant on PES.

Experimentally, the rate constant of the title reaction was measured to be $(5.4 - 8.8) \times 10^{-13}$ cm^3 molecule^{-1} s^{-1} for total pressures 2.0 – 15.5 Torr of N_2 and confirmed the reaction proceeds by the three-body process. Form the result of calculations we can presume, with the barrier of 27.3 kcal/mol and the high energy of TS2 which is only 2.0 kcal/mol above reactant, it is conceivable that the title reaction is relative slow compared with the reaction of oxygen and active radicals,

Table 1 The relative and total energies and ZPE at B3LYP and G3MP2//B3LYP levels for the reaction of NCCO + O_2 (E_T and ZPE in hartree, E_R in kcal/mol)

Species	B3LYP		G3MP2//B3LYP		ZPE
	E_T	E_R	E_T	E_R	
R:NCCO + O_2	−356.4900	0.0	−356.0100	0.0	0.01753
P1:NCO + CO_2	−356.6694	−112.6	−356.1939	−115.4	0.02172
P2:CNO + CO_2	−356.5699	−50.2	−356.0933	−52.3	0.02055
P3:NCO + CO + O	−356.4666	14.7	−355.9934	10.4	0.01506
P4:CO_2 + CN + O	−356.4468	27.17	−355.9808	18.3	0.01662
P5:CO + ONCO	−356.5780	−55.27	−356.1010	−57.1	0.01813
P6:2CO + NO	−356.4900	−71.9	−356.1447	−84.6	0.01465
IM1	−356.5269	−23.2	−356.0567	−29.3	0.02283
IM2	−356.5265	−22.92	−356.0556	−28.7	0.02289
IM3	−356.5076	−11.02	−356.0376	−17.3	0.02340

Table 1 continued

Species	B3LYP		G3MP2//B3LYP		ZPE
	E_T	E_R	E_T	E_R	
IM4	−356.4656	15.3	−355.9963	8.6	0.02354
IM5	−356.4673	14.2	−355.9678	26.4	0.02268
IM6	−356.4580	20.1	−355.9832	16.8	0.02043
IM7	−356.4466	27.2	−355.9798	18.9	0.02311
IM8	−356.5502	−37.8	−356.0685	−36.8	0.02140
IM9	−356.5285	−24.2	−356.0504	−25.4	0.02296
IM10	−356.5427	−33.1	−356.0538	−27.5	0.02240
IM11	−356.5767	−54.4	−356.1090	−62.2	0.02385
IM12	−356.5140	−15.1	−356.0284	−11.6	0.02020
IM13	−356.5098	−12.4	−356.0441	−21.4	0.02292
IM14 + O	−356.4677	14.0	−355.9893	12.9	0.01950
IM15 + O	−356.4954	−3.4	−356.0138	−2.4	0.01970
IM16 + O	−356.4509	24.5	−355.9715	24.1	0.01842
IM17 + O	−356.4509	24.5	−355.9646	28.4	0.01868
IM18 + CO	−356.5612	−44.7	−356.0957	−53.8	0.01855
IM19 + CO_2	−356.5391	−30.8	−356.0700	−37.7	0.01853
IM20 + CO	−356.4077	51.6	−355.9453	40.6	0.01771
TS1	−356.5163	−16.5	−356.0443	−21.6	0.02224
TS2	−356.4866	2.1	−356.0131	−2.0	0.02123
TS3	−356.4935	−2.2	−355.9970	8.1	0.02013
TS4	−356.4594	19.2	−355.9881	13.7	0.02180
TS5	−356.4596	19.1	−355.9809	18.2	0.02129
TS6	−356.4572	20.6	−355.9494	38.0	0.02117
TS7	−356.4328	35.9	−355.9363	46.2	0.01976
TS8	−356.4499	25.1	−355.9624	29.8	0.01833
TS9	−356.4433	29.3	−355.9621	30.0	0.01980
TS10	−356.4145	47.4	−355.9317	49.1	0.02004
TS11	−356.4397	31.5	−355.9690	25.7	0.02117
TS12	−356.5241	−21.4	−356.0436	−21.1	0.02204
TS13	−356.5331	−27.1	−356.0542	−27.8	0.02044
TS14	−356.5457	−35.0	−356.0668	−35.7	0.01882
TS15	−356.5398	−31.3	−356.0563	−29.1	0.01834
TS16	−356.5267	−23.0	−356.0482	−24.0	0.02186
TS17	−356.5375	−29.8	−356.0545	−28.0	0.02149
TS18	−356.4952	−3.3	−356.0238	−8.7	0.02050
TS19	−356.5129	−14.4	−356.0011	5.5	0.01994
TS20	−356.4937	−2.3	−356.0178	−4.9	0.01945
TS21	−356.5000	−6.3	−356.0303	−12.8	0.02008
TS22	−356.4967	−4.2	−356.0299	−12.5	0.02122
TS23	−356.4064	52.4	−355.9419	42.7	0.01857
TS24 + O	−356.4668	14.5	−355.9890	13.1	0.01874
TS25 + O	−356.4657	15.2	−355.9881	13.7	0.01646
TS26 + O	−356.4018	55.3	−355.9288	50.9	0.01703
TS27 + O	−356.4244	41.1	−355.9510	37.0	0.01668
TS28 + O	−356.4333	35.6	−355.9546	34.7	0.01637
TS29 + CO_2	−356.5140	−15.1	−356.0389	−18.2	0.01777
TS30 + CO	−356.5563	−41.6	−356.0872	−48.5	0.01749
TS31 + CO	−356.4064	52.4	−355.9417	42.8	0.01574

and it is more prefer to deactivate through collision, and this supposition is agreement with the conclusion of experiment. Compared with the reaction of O_2 with HCCCCO which is the isoelectronic of NCCO, the major product are $HCCO + CO_2$, and this is accordance with the title reaction.

4 Conclusions

In this paper, the theoretical study gives some insights into the mechanisms of the $NCCO + O_2$ reaction at the G3MP2// B3LYP/6-311G(d,p) level. The calculations show that two mechanisms are involved, namely, α-C atom addition mechanism and β-C atom addition mechanism, and three possible attack ways are considered. With the energy-rich initial adduct of IM1 and without entrance barrier, the former mechanism is predominant over the latter one. With the abundant energy available from IM1, and lower barrier demanded, and the most stable product, the most feasible and simplest channel is $R \rightarrow IM1 \rightarrow TS2 \rightarrow IM3 \rightarrow TS3 \rightarrow P1(NCO + CO_2)$. For other products such as $CNO + CO_2$, $CO_2 + CN + O$, $NCO + CO + O$, and $CO + ONCO$ are less important.

References

1. Reisler HS, Mangir M, Wittig C (1980) J Chem Phys 73:2280
2. Krause HF (1979) J Chem Phys 70:3871
3. Le QN, Vanpee M (1985) Combust Flame 62:193
4. Williams BA, Pasternack L (1997) Combust Flame 111:87
5. Kruse T, Roth P (1999) Int J Chem Kinet 31:11
6. Becker KH, Donner B, Schmidt F, Wiesen PZ (2000) Phys Chem 214:503
7. Ristanovic A, Fernandez A, Fontijn A (2002) J Phys Chem A 106:8291
8. Kruse T, Roth P (1999) Int J Chem Kinet 31:11
9. Furlan A, Scheld HA, Huber JR (1998) Chem Phys Lett 282:1
10. Sumiyoshi Y, Takada H, Endo Y (2004) Chem Phys Lett 387:116
11. Francisco JS, Liu RF (1997) J Chem Phys 107:3840
12. Yu GT, Ding YH, Huang XR, Sun CC (2005) J Chem Phys A 109:2364
13. Jursic BS (1999) J Mol Struct (THEOCHEM) 460:207
14. Imamura T, Washida N (2000) Int J Chem Kinet 11:440
15. Curtiss LA, Raghavachari K, Redfern PC, Pople JA (1998) J Chem Phys 109:7764
16. Baboul AG, Curtiss LA, Raghavachari K (1999) J Chem Phys 110:7650
17. Frisch MJ, Trucks GW, Schlegel HB, Scuseria GE, Robb MA, Cheeseman JR, Zakrzewski VG., Montgomery JA, Stratmann RE, Burant JC, Dapprich S, Millam JM, Daniels AD, Kudin KN, Strain MC, Farkas O, Tomasi J, Barone V, Cossi M, Cammi R, Mennucci B, Pomelli C, Adamo C, Clifford S, Ochterski J, Petersson GA, Ayala PY, Cui Q, Morokuma K, Malick DK, Rabuck AD, Raghavachari K, Foresman JB, Cioslowski J, Ortiz JV, Stefanov BB, Liu G, Liashenko A, Piskorz P, Komaromi I, Gomperts R, Martin RL, Fox DJ, Keith T, Al-Laham MA, Peng CY, Nanayakkara A, Gonzalez C, Challacombe M, Gill PMW, Johnson BG, Chen W, Wong MW, Andres JL, Head-Gordon M, Replogle ES, Pople JA (1998) Gaussian 98, revision A.9. Gaussian, Pittsburgh